Springer

KSME

Journal of Mechanical Science and Technology 25 (5) (2011) 1279~1286
www.springerlink.com/content/1738-494x
DOI 10.1007/s12206-011-0231-4

Detection of faults in gearboxes using acoustic emission signal †

DongSik Gu[1], JaeGu kim[1], YoungSu An[2] and ByeongKeun Choi[3,*]

[1]*Department of Precision and Mechanical Engineering, Gyeongsang National University, 445 Inpyeong-dong, Tongyoung city, Gyeongnam-do, 650-160, Korea*
[2]*The Training Ship Management Center, Institute of Marine Industry, Gyeongsang National University, 445 Inpyeong-dong, Tongyoung city, Gyeongnam-do, 650-160, Korea*
[3]*Department of Energy and Mechanical Engineering, Institute of Marine Industry, Gyeongsang National University, 445 Inpyeong-dong, Tongyoung city, Gyeongnam-do, 650-160, Korea*

(Manuscript Received September 28, 2010; Revised February 9, 2011; Accepted February 14, 2011)

Abstract

Vibration analysis is widely used in machinery diagnosis, and wavelet transform and envelope analysis have also been implemented in many applications to monitor machinery condition. Envelope analysis is well known as a useful tool for the detection of rolling element bearing faults, and wavelet transform is used in research to detect faults in gearboxes. These are applied for the development of the condition monitoring system for early detection of the faults generated in several key components of machinery. Early detection of the faults is a very important factor for condition monitoring and a basic component to extend CBM (Condition-Based Maintenance) to PM (Prediction Maintenance). The AE (acoustic emission) sensor has a specific characteristic on the high sensitivity of the signal, high frequency and low energy. Recently, AE technique has been applied in some studies for the early detection of machine fault. In this paper, a signal processing method for AE signal by envelope analysis with discrete wavelet transforms is proposed. Through the 15 days test using AE sensor, misalignment and bearing faults were observed and early fault stage was detected. Also, in order to find the advantage of the proposed signal processing method, the result was compared to that of the traditional envelope analysis and the accelerometer signal.

Keywords: Acoustic emission (AE) technique; Fault detection; Gearboxes; Wavelet transform; Envelope analysis; Early detection; Condition monitoring

1. Introduction

Application of the high-frequency acoustic emission (AE) technique in condition monitoring of rotating machinery has been growing over recent years. This is particularly true for bearing defect diagnosis and seal rubbing [1-8]. The main drawback with the application of the AE technique is the attenuation of the signal and as such the AE sensor has to be close to its source. However, it is often practical to place the AE sensor on the non-rotating member of the machine, such as the bearing or gear casing. Therefore, the AE signal originating from the defective component will suffer severe attenuation before reaching the sensor. Typical frequencies associated with AE activity range from 20 kHz to 1 MHz.

While vibration analysis on gear fault diagnosis is well established, the application of AE to this field is still in its infancy. In addition, there are limited publications on the application of AE to gear fault diagnosis. Siores et al. [9] explored several AE analysis techniques in an attempt to correlate all possible failure modes of a gearbox during its useful life. Failures such as excessive backlash, shaft misalignment, tooth breakage, scuffing, and a worn tooth were seeded during tests. Siores correlated the various seeded failure modes of the gearbox with the AE amplitude, root mean square, standard deviation and duration. It was concluded that the AE results could be correlated to various defect conditions. Sentoku [10] correlated tooth surface damage, such as pitting, to AE activity. An AE sensor was mounted on the gear wheel and the AE signature was transmitted from the sensor to data acquisition card across a mercury slip ring. It was concluded that AE amplitude and energy increased with increased pitting. In a separated study, Singh et al. [11] studied the feasibility of AE for gear fault diagnosis. In one test, a simulated pit was introduced on the pitch line of a gear tooth using an electrical discharge machining (EDM) process. An AE sensor and an accelerometer for comparative purposes were employed in both test cases. It was important to note that both the accelerometer and AE sensor were placed on the gearbox casing. It was observed that the AE amplitude increased with increased rotational speed and increased AE activity was observed with increased pitting. In a second test, periodically occurring peaks were observed when natural pitting started to appear

† This paper was recommended for publication in revised form by Associate Editor Ohseop Song

* Corresponding author. Tel.: +82 55 772 9116, Fax.: +82 55 772 9119
E-mail address: bgchoi@gnu.ac.kr

after half an hour of operation. These AE activities increased as the pitting spread over more teeth. Singh et al. [11] concluded that AE could provide earlier detection over vibration monitoring for pitting of gears, but noted it could not be applicable to extremely high speeds or for unloaded gear conditions. Tan et al. [12] offered that AE rms levels from the pinion were linearly correlated to pitting rates; AE showed better sensitivity than vibration at a higher torque level (220 Nm) due to fatigue gear testing using spur gears. He made sure that the linear relationship between AE, gearbox running time and pit progression implied that the AE technique offers good potential in prognostic capabilities for monitoring the health of rotating machines.

On the other hand, the signal processing method for AE signal was studied using bearing and gearbox. In the results of the research [13-15], the envelope analysis was found to be useful to detect fault in rolling element bearing. The fault detection frequency of bearing can be presented in the power spectrum. Wavelet transform was used for the signal processing method for the gearboxes [16, 17], but wavelet transforms can give the different results with the envelope analysis. It can show the defect frequency, but the efficiency is lower than that of envelope analysis. Thus, the signal processing method for AE signal has not been completed until now, and it must be developed in the future. Therefore, in this paper, a signal processing method for AE signal by envelope analysis with discrete wavelet transforms is proposed. For the detection of faults generated by gear systems using the suggested signal processing, a gearbox was installed in the test rig system. Misalignment was created by a twisted case caused by arc-welding to fix the base, and bearing inner race fault was generated by severe misalignment. Through the 15 days test using AE sensor, misalignment was observed and bearing faults were also detected in the early fault stage. To identify the sensing ability of the AE, vibration signal was acquired through an accelerometer and compared with the AE signal. Also, to find the advantage of the proposed signal processing method, it was compared to traditional envelope analysis. The detection results of the test were shown by the power spectrum and comparison of the harmonics level of the rotating speed. Modal test and zooming by a microscope were performed to prove the reason of the other faults.

2. Proposition of signal processing

Envelope analysis typically refers to the following sequence of procedures: (1) band-pass filtering (BPF), (2) wave rectification, (3) Hilbert transform or low-pass filtering (LPF) and (4) power spectrum. The purpose of the band-pass filtering is to reject the low-frequency high-amplitude signals associated with the *i* th mechanical vibration components and to eliminate random noise outside the pass-band. Theoretically, in HFRT (High Frequency Resonance Technique) analysis, the best band-pass range includes the resonance of the bearing components. This frequency can be found through impact tests or theoretical calculations involving the dimensions and material properties of the bearing. However, it is very difficult to predict or specify which resonant modes of neighboring structures will be excited. It will be costly and unrealistic in practice to find the resonant modes through experiments on rotating machinery that may also alter under the different operational conditions. In addition, it is also difficult to estimate how these resonant modes are affected in the assembly of a complete bearing and mounting in a specific housing, even if the resonant frequencies of individual bearing elements can be tested or calculated theoretically [18]. Therefore, most researchers decide on the band-pass range as on option. To recover the disadvantages of this option, discrete wavelet transform (DWT) is included in the process of traditional envelope analysis in this paper.

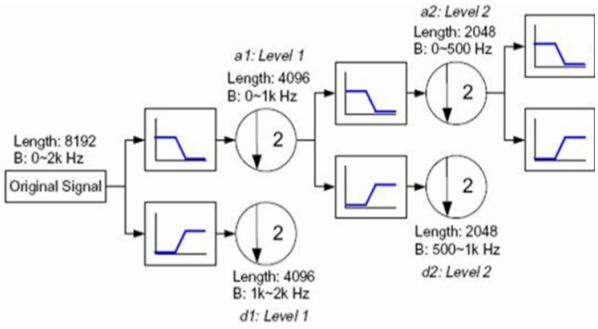

Fig. 1. Wavelet decomposition tree [18].

In the DWT, the approximate coefficients and detail coefficients decomposed from a discredited signal can be expressed as

$$a_{(j+1),k} = \sum_{k=0}^{N} a_{j,k} \int \phi_{j,k}(t) \cdot \phi_{(j+1),k}(t) dt = \sum_{k} a_{j,k} \cdot g[k] \quad (1)$$

$$d_{(j+1),k} = \sum_{k=0}^{N} a_{j,k} \int \phi_{j,k}(t) \cdot \varphi_{(j+1),k}(t) dt = \sum_{k} a_{j,k} \cdot h[k]. \quad (2)$$

The decomposition coefficients can therefore be determined through convolution and implemented by using a filter. The filter, $g[k]$, is a low-pass filter and is a high-pass filter. The decomposition process can be iterated, with successive approximations being decomposed in turn, so that one signal is broken down into many lower resolution components. This is called the wavelet decomposition tree, as shown in Fig. 1.

DWT has a de-noise function and a filter effect focused on impact signal. To make up the weak point of BPF of the envelope analysis, DWT was intercalated on typical envelope analysis, between BPF and wave rectification exactly. The signal by DWT will be separated to different band widths by decomposition level and adapted to the signal with impact.

For more complicated signals, which are expressible as a sum of many sinusoids, a filter can be constructed which shifts each sinusoidal component by a quarter cycle. This is called a Hilbert transform filter. Let $Ht\{x\}$ denote the output at time t of the Hilbert-transform filter applied to the signal x. Ideally, this filter has magnitude 1 at all frequencies and introduces a

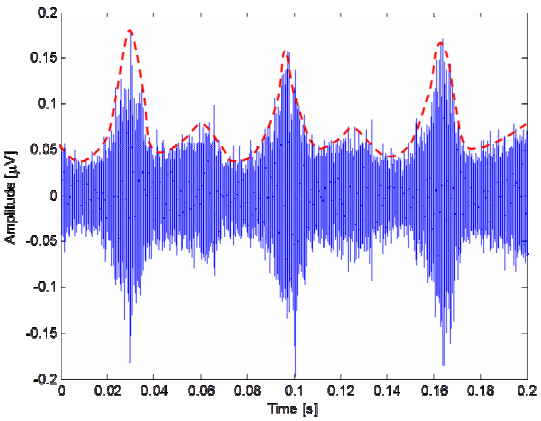

Fig. 2. Analytic signal (dash) of the envelope effect.

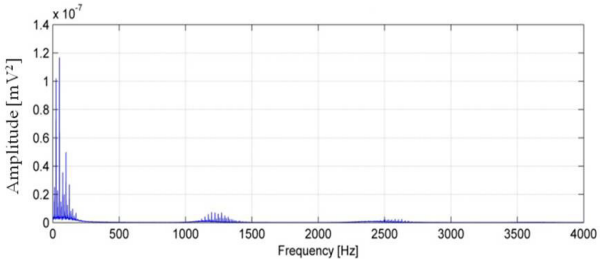

(a) Envelope analysis

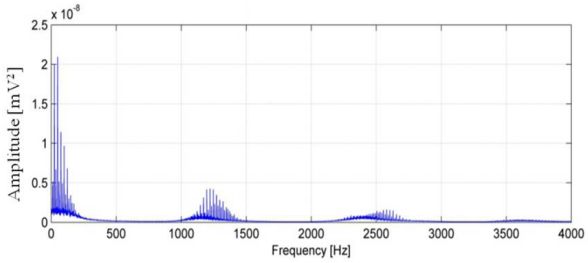

(b) Envelope analysis with DWT

Fig. 3. The comparison of power spectrums in envelope analysis with/without DWT.

phase shift of $-\pi/2$ at each positive frequency and $+\pi/2$ at each negative frequency. When a real signal $x(t)$ and its Hilbert transform $y(t) = Ht\{t\}$ are used to form a new complex signal $z(t)= x(t)+jy(t)$, the signal $z(t)$ is the (complex) analytic signal corresponding to the real signal $x(t)$. In other words, for any real signal $x(t)$, the corresponding analytic signal $z(t) = x(t)+jHt\{x\}$ has the property that all 'negative frequencies' of $x(t)$ have been 'filtered out' [19]. Hence, the coefficients of the complex term in the corresponding analytic signal were used for FFT.

Fig. 2 shows an analytic signal of the Hilbert transform for envelope analysis. The solid line is a time signal and the dash is its envelope curve. A high frequency signal modified by wavelet transform is modulated to a low frequency signal with no loss of the fault information due to envelope effect. According to that, the fault signals in the low frequency region can be detected using the analytic signal. That is an important fact for the proposed signal processing method.

Therefore, the proposed signal processing method in this paper is an envelope analysis with DWT and using the coefficients of the complex term in Hilbert transform.

Furthermore, to reduce the noise level in the power spectrum, the spectrum values were presented as the mean value of each day. Fig. 3 shows the power spectrums of the two different signal processing methods. Fig. 3(a) is from envelope analysis, and Fig. 3(b) shows the envelope analysis intercalated DWT using Daubechies mother function between BPF and wave rectification. In Fig. 3, the DWT has an effect the amplifying sidebands peaks, especially about gear mesh frequencies, so the peaks of the harmonics of the rotating speed (f_r) and gear mesh frequencies (f_m) are bigger than another, and we can check them easily. Therefore, in the following result, the power spectrum through envelope analysis with DWT will be shown.

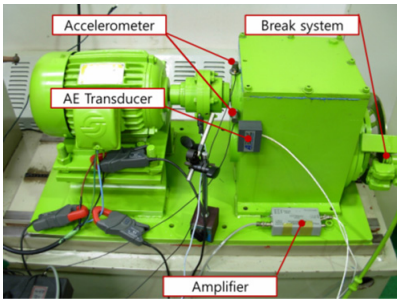

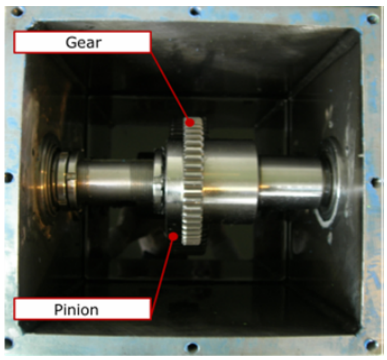

Fig. 4. Test-rig.

3. Experimental setup

3.1 Test-rig

The test-rig employed for this investigation consists of one identical oil-bath lubricated gearbox, 3 HP-motor, rigid coupling, tapper-roller bearing, pinion, gear, control panel and break system, as seen Fig. 4. The pinion was made from steel with heat treatment, the number of teeth is 70, and diameter is 140 mm. The gear was made from steel, but it was produced without any heat treatment process during manufacturing. The number of gear teeth is 50, and diameter is 100 mm and module is 2 mm for the gear and pinion, respectively.

Table 1. Specification of gearbox and bearing.

	Gear		Pinion	
No. of teeth	50		70	
Speed of shaft	25.01 rev/s			
Meshing frequency	1250 Hz		1750 Hz	
Bearing (NSK HR 32206J)				
No. of rolling element	17	Type	Defect Freq. (f_d)	Fault Freq. (f_d X f_r)
Diameter of outer race	62 mm	BPFO	8.76 Hz	219.3 Hz
		BPFI	11.24 Hz	281.38 Hz
Diameter of inner race	30 mm	FTF	3.84 Hz	96.13 Hz
		BSF	0.44 Hz	11.01 Hz

BPFO : ball pass frequency of outer race
BPFI : ball pass frequency of inner race
FTF : fundamental train frequency
BSF : ball spin frequency

Table 2. Specifications of data acquisition system.

2 Channel AE system on PCI-Board	18-bit A/D conversion 10M samples/s rate (on one channel, 5M samples/s on 2 AE channels)
AE Sensor (Wideband type)	Peak sensitivity V/(m/s);[V/μbar] : 55[-62] dB Operating frequency range : 100-1,000 kHz Directionality : ±1.5 dB
Preamplifier Gain	Wide dynamic range < 90 dB Single power/signal BNC or optional separate power/signal BNC 20/40/60 dB selectable gain

A simple mechanism that permitted a break of disk-pad type to be rotated relative to each other was employed to apply torque to the gear. Contact ratio (Pinion / Gear) of the gears was 1.4. The motor used to drive the gearbox was a 3-phase induction motor with a maximum running speed of 1800 rpm and was operated for 15 days with 1500 rpm. The torque on the output shaft was 1.2 kN · m while the motor was in operation, and other specifications of the gearbox are given as in Table 1.

3.2 Acquisition system and test procedures

AE sensors used in this paper are a broadband type with a relative flat response in the range frequency from 100 kHz to 1 MHz. They are placed on the right side of the gearbox cases near the coupling in the horizontal direction at the same height with the shaft center (Fig. 4).

AE signals are pre-amplified by 60 dB and the output from the amplifier is collected by a commercial data acquisition card with 10 MHz sampling rate during the test. Prior to the analog-to-digital converter (ADC), anti-aliasing filter is employed that can be controlled DAQ software. Table 2 shows the detailed specifications of the data acquisition system.

Before the test, attenuation test on the gearbox components was taken in order to understand the characteristics of the test-rig. The gearbox was run for 30 minutes prior to acquiring AE data for the unload condition. Based on the sampling rate of 10 MHz, the available recording acquisition time was 2 sec.

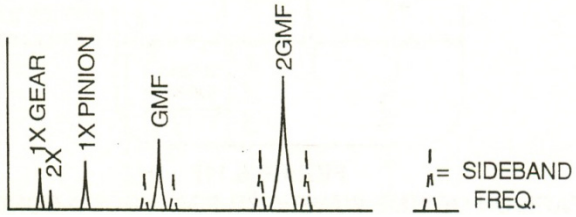

Fig. 5. Spectrum indicating misalignment of gear (GMF = fm)[20].

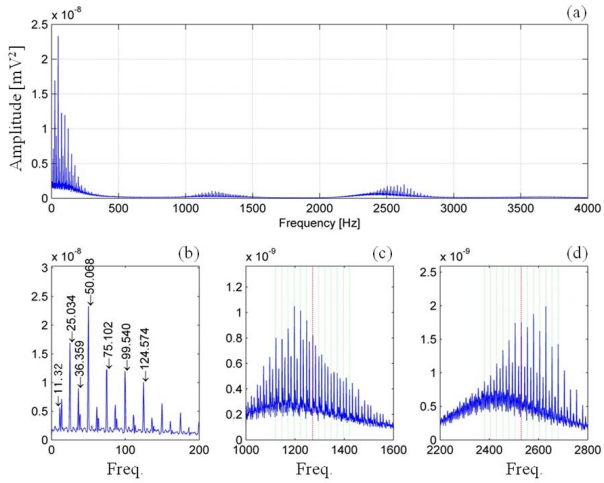

Fig. 6. Power spectrum of the second day.

4. Experiment result and discussion

In general, the misaligned gear which almost always excites higher order f_m harmonics is shown as in Fig. 5. Often, only small amplitudes will be at the fundamental f_m, but much higher levels will be at $2f_m$ and/or $3f_m$. The sideband spacing about f_m might be $2f_r$ or even $3f_r$ when gear misalignment problems are involved. When significant tooth wear occurs, not only will sidebands appear about f_m, but also about the gear natural frequencies. In the case of those around f_m, the amplitude of the sidebands themselves is a better indicator for wear than the amplitude of f_m.

As for significant gear eccentricity and/or backlash, these problems display the following characteristics:

- Both eccentricity and backlash excite the gear natural frequencies as well as f_m. They also may generate a number of sidebands about both the natural and gear mesh frequencies.
- If a gear is eccentric, it will modulate the natural frequency and gear mesh frequencies, both of which will be sidebanded around f_r of the eccentric gear. An eccentric gear can generate significant forces, stresses and vibration if it is forced to bottom out with the meshing gears [20].

In the results of the envelop analysis with DWT, the high harmonics of f_m occurred by strong wearing phenomena caused by misaligned teeth. In the power spectrum (Fig. 6), 25Hz (f_r) and its harmonics are generated and 11.32Hz was the ball pass frequency of inner race (BPFI [f_d]). In Fig. 6(c) and

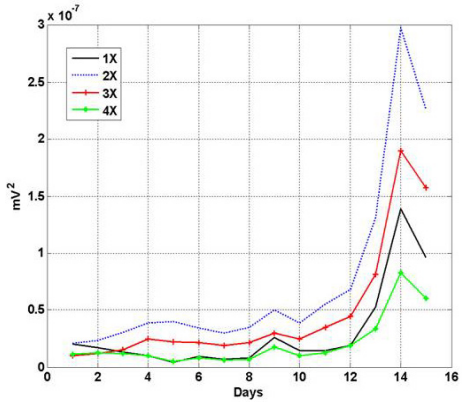

(a) Harmonics of the rotating speed

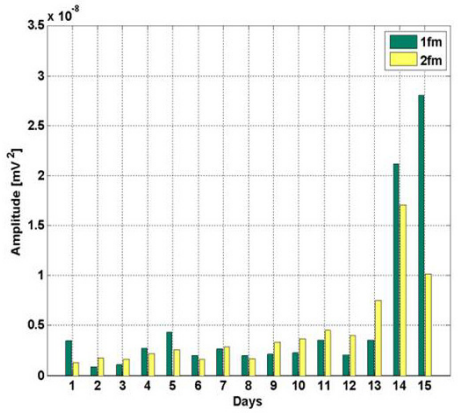

(b) Harmonics of the gear mesh frequency

Fig. 7. Peak level trend along days.

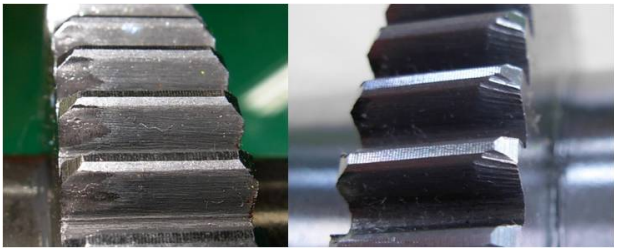

Fig. 8. Gear tooth weaned by misalignment.

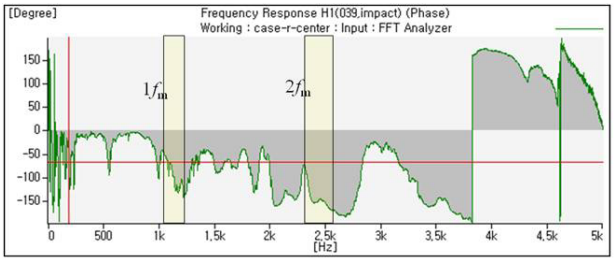

(a) Phase

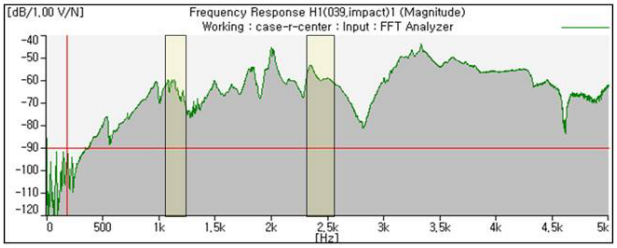

(b) Frequency response function

Fig. 9. Modal test result.

(d), the center dash line is shown for f_m and $2f_m$, and their side lines are the sidebands with difference 25Hz (f_r).

In condition monitoring for general rotating machinery, the harmonics ($2f_r$, $3f_r$, $4f_r$, $\cdots$) of f_r occurred higher than f_r when the misalignment happened. According to the phenomena of misalignment as shown in Fig. 5, high level harmonics of f_r were generated such as in Fig. 6(b), and $2f_r$ was always bigger than f_r as shown in Fig. 7(a). The level of $2f_m$ from second to thirteenth day was higher than or similar to f_r as shown in Fig. 7(b). Thus, it is easily catching up to the misalignment that occurred in this test rig. However, it might be that faults of this system are not only misalignment but also resonance trouble, looseness, bearing fault, etc.

Wearing effect by misalignment pollutes the lubrication oil. In Fig. 8, it could be found by the worn teeth and the spots near the pieces of gear teeth. The dripped pieces from the unloading surface raised the wearing effect on the loading surface, then the gap between gear and pinion was increased. In addition, we could know that the impact marks on the unloading surface (Fig. 8(b)) were generated by misalignment; the impacting force was strong in the initial condition. In this way, the gear teeth were seriously damaged as in Fig. 8. In Fig. 6(c) and (d), the sidebands are created on wide-spread frequency range near f_m and $2f_m$. That is similar to a state excited by impact force. To confirm the natural frequencies of the test-rig, a modal test was fulfilled. The result of the modal test for the gearbox, as in Fig. 9, show that f_m and $2f_m$ exist on the exiting frequency range. On the other hand, partial frequency bands close to f_m and $2f_m$ were excited by the impact force, but it is not an exact natural frequency because the phase did not shift enough. Therefore, the peaks near f_m and $2f_m$ were amplified and have many sidebands of f_r and 11.32Hz (BPFI [f_d]). Therefore, it is considered that excessive backlash occurred. Moreover, Fig. 10(a) shows the zooming power spectrum of Fig. 6(a) focused on f_r harmonics. We could clearly know that if the sidebands were caused by BPFI [f_d], then the inner race had some kind of fault. To find out the fault, the surface of the bearing inner race was carried out and viewed by a microscope with 100X zoom as shown in Fig. 11. Small spots were found on the surface, and small cracks were found out on the spots. However, this trouble was not seeded and existed from the initial condition. Thus, it is as assumed that the problem happened in assembly and/or was caused by misalignment.

To identify the sensing ability of the AE, vibration signal was acquired through accelerometer and compared with the AE signal. Also, to find the advantage of the proposed signal processing method, it was compared to traditional envelope analysis.

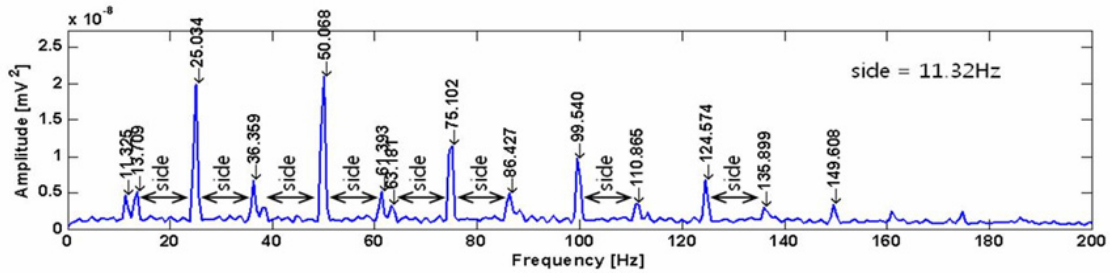

(a) Power spectrum of the AE signal using envelope analysis with DWT(suggested)

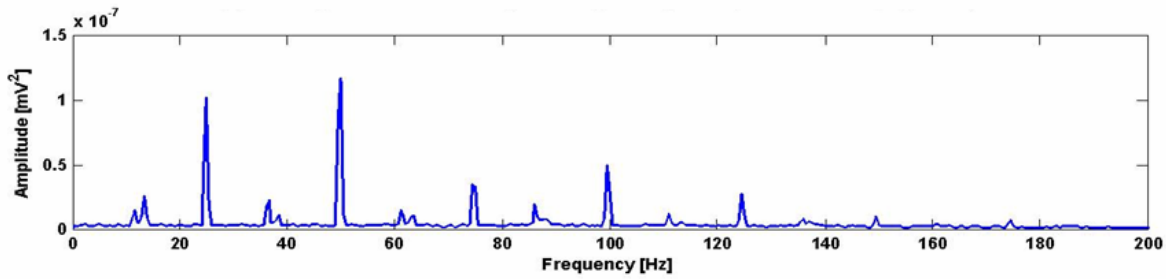

(b) Power spectrum of the AE signal using traditional envelope analysis

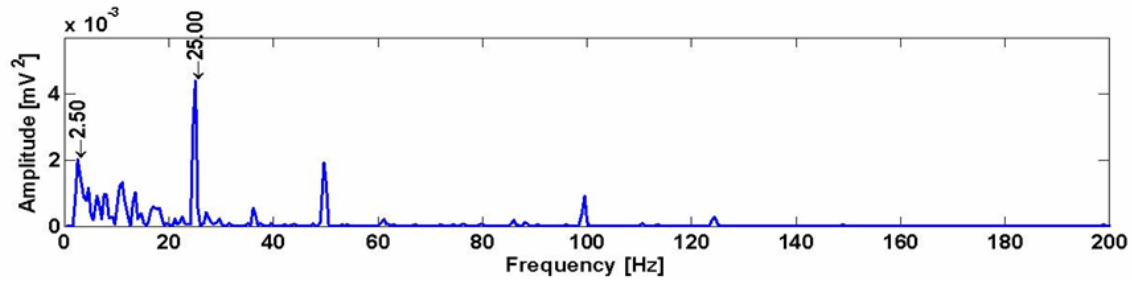

(c) Power spectrum of the signal from accelerometer

Fig. 10. Sidebands BPFI in the first day power spectrum.

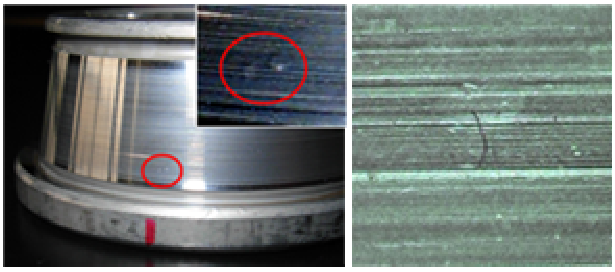

Fig. 11. Zooming of the inner race surface of the fault bearing.

The power spectrum of the AE signal using traditional envelope analysis is shown in Fig. 10(b), and the power spectrum using the vibration signal by accelerometer is displayed in Fig. 10(c). The vibration signal was treated by the same method with AE signal. The harmonics of f_r are generated, and $2f_r$ for detecting the misalignment is created and can be found in all spectrums (Fig. 10), but the power spectrum of the AE signal, Fig. 10(a) and (b), can explicitly display the defect frequencies as compared to the accelerometer signal (Fig. 10(c)). For example, in Fig. 10(c), the sidebands of BPFI are not easily found because of the higher level of noise in the low frequency range below f_r than in the AE signal with or without DWT.

According to the above results, we can understand that the AE signal can detect the fault more easily than accelerometers and can be used in the condition monitoring system for early detection fault. Moreover, as shown in Table 3, which is the ratio of peaks versus the maximum peak in the respective spectrum, the peak levels of the harmonics of f_r and sidebands caused by BPFI are highly generated in the proposed signal processing method (Fig. 10(a)) than the traditional method. This can lead good feature values to evaluate the condition of the machinery. Therefore, the power spectrum of the proposed envelope analysis using AE signal can be shown the clean result with harmonics and sidebands and is a better technique for condition monitoring system.

Table 3. Ratio of peaks versus the maximum peak in respective spectrum.

Frequency [Hz]		Traditional Method [%]	Proposed method [%]
13.709	1X-BPFI	0.2146	0.2459
25.034	1X	0.8727	0.9525
36.360	1X+BPFI	0.1936	0.3196
38.750	2X- BPFI	0.0952	0.1435
50.070	2X	1.0000	1.0000
61.393	2X+ BPFI	0.1277	0.2470
63.181	3X- BPFI	0.0970	0.1560
75.102	3X	0.3044	0.5465
86.427	3X+ BPFI	0.1699	0.2352
99.540	4X	0.4269	0.4616
110.866	4X+ BPFI	0.1062	0.1675
124.574	5X	0.2312	0.3253
135.899	5X+ BPFI	0.0714	0.1443

5. Conclusions

In this paper, a signal processing method for AE signal by envelope analysis with discrete wavelet transforms is proposed. For the detection of faults generated from a gear system using the suggested signal processing, a gearbox was installed in the test rig system. Misalignment was created by twisted case caused by arc-welding to fix the base, and bearing inner race fault is generated by severe misalignment. To identify the sensing ability of the AE, vibration signal was acquired through accelerometer and compared to the AE signal. Also, to find the advantage of the proposed signal processing method, it was compared with traditional envelope analysis.

According to the experiment result, AE sensor can detect the fault earlier than an accelerometer because of high sensitivity, and in the power spectrum, the harmonics of the rotating speed and the gear mesh frequency clearly occurred. Misalignment was observed and bearing faults were also detected in the early fault stage. The proposed envelope analysis is worked to evaluate the faults and indicated the faults frequencies, rotating speed, sideband of BPFI, gear mesh frequency and harmonics, explicitly.

Therefore, for condition monitoring of the machinery, the AE system is a powerful method to detect faults earlier, and the proposed signal processing method, that is the envelope analysis intercalated DWT using Daubechies mother function between BPF and wave rectification, can be shown to provide better result than traditional envelope analysis.

Acknowledgment

This work has been supported by the oversea research program of GNU and the 2nd Phase of Brain Korea 21.

References

[1] P. D. Mba and R. H. Bannister, Condition monitoring of low-speed rotating machinery using stress waves: Part 1 and Part 2, *Proc. IMechE* 213(3, Part E), (1999) 153-185.

[2] T. Holroyd and N. Randall, The use of acoustic emission for machine condition monitoring, *Br. J. Non-Destruct Test* (1992) 75.

[3] D. Mba, The detection of shaft-seal rubbing in large-scale turbines using acoustic emission, *14th International Congress on Condition Monitoring and Diagnostic Engineering Management,* Manchester, UK, 4-6 Sept. (2001) 21-28.

[4] D. Mba, A. Cooke, D. Roby and G. Hewitt, Opportunities offered by acoustic emission for shaft-steal rubbing in power generation turbines: A case study, *Int. Conf. on Condition Monitoring* (2003) 280-286.

[5] Y. H. Kim, A. C. C. Tan, J. Mathew, V. Kosse and B. S. Yang, A comparative study on the application of acoustic emission technique and acceleration measurements for low speed condition monitoring, *12th Asia-Pacific Vibration Conference,* 6-9 August, Hokkaido Univ., Japan (2007).

[6] Y. H. Kim, A. C. C. Tan, J. Mathew and B. S. Yang, Experimental study on incipient fault detection of low speed rolling element bearings: time domain statistical parameters, *12th Asia-Pacific Vibration Conference,* 6-9 August, Hokkaido Univ., Japan (2007).

[7] C. K. Tan and D. Mba, Limitation of acoustic emission for identifying seeded defects in gearboxes, *Journal of Non-Destructive Evaluation*, 24 (1) (2005) 11-28.

[8] E. Siores and A. A. Negro, Condition monitoring of a gear box using acoustic emission testing, *Material Evaluation*, (1997) 183-187.

[9] H. Sentoku, AE in tooth surface failure process of spur gear, *J. Acoustic Emission*, 16 (1-4) (1998) S19-S24.

[10] A. Singh, D. R. Houser and S. Vijayakar, Early detection of gear pitting, *Power Trans. Gear. Conf. SAME. DE88* (1996) 673-678.

[11] J. Shiroshi, Y. Li, S. Lian, S. Danyluk and T. Kurfess, Vibration analysis for bearing outer race condition diagnostics, *Presented at Journal of Brazilian Society of Mechanical Science,* 21 (3) (1999).

[12] C. K. Tan, P. Irving and D. Mba, A comparative experimental study on the diagnostic and prognostic capabilities of acoustics emission, vibration and spectrometric oil analysis for spur gears, *Mechanical Systems and Signal Processing*, 21 (2007) 208-233.

[13] Y. T. Sheen, An envelope analysis based on the resonance modes of the mechanical system for the bearing defect diagnosis, *Measurement*, 43 (7) (2010) 912-934.

[14] Y. Yang, D. Yu, J. Cheng, A fault diagnosis approach for roller bearing based on IMF envelope spectrum and SVM, *Measurement*, 40 (9-10) (2007) 943-950.

[15] Y. T. Sheen, An envelope detection method based on the first-vibration-mode of bearing vibration, *Measurement*, 41 (7) (2008) 797-809.

[16] J. D. Wu, C. C. Hsu and G. Z. Wu, Fault gear identifiction and classification using discrete wavelet transform and adaptive neuro-fuzzy inference, *Expert Systems with Applications*, 36 (3) (2009) 6244-6255.
[17] J. D. Wu and J. C. Chen, Continuous wavelet transform technique for fault signal diagnosis of internal combustions engines, *NDT&E International*, 39 (4) (2006) 304-311.
[18] M. Misiti, Y. Misiti, G. Oppenheim and J. M. Poggi, *Wavelet Toolbox TM 4 user's guide*, The MathWorks Inc., Natick, USA (2009).
[19] H. Douglas and P. Pillay, The impact of wavelet selection on transient motor current signature analysis, *Proceedings of IEEE international conference on Electrical Machine and Drives* (2005) 80-85.
[20] E. James and P. E. Bery, *IRD advancement training analysys II*, IRD Mechananalysis Inc., Ohio, USA (1994).
[21] K. M. Ronnie and V. K. Eric, *Nondestructive testing handbook*, volume 6, American Society for nondestructive testing, Ohio, USA (2005).
[22] H. Li, Y. Zhang and H. Zheng, Gear fault detection and diagnosis under speed-up condition based on order cepstrum and radial basis function neural network, *Journal of Mechanical Science and Technology*, 23 (2009) 2780-2789.
[23] C. S. Burrus, R. A. Gopinath and H. Guo, *Introduction to wavelet and wavelet transforms*, Prentice-Hall, Upper Saddle River, USA (1998).

DongSik Gu received B.S. degree in Division of Mechanical and Aerospace Engineering from Gyeongsang National University, Korea. Mr. Gu is currently a Unified Master's and Doctor's Course from Department of Precision and Mechanical Engineering, Gyeongsang National University, Korea.

JaeGu Kim received B.S. degree in Division of Mechanical and Aerospace Engineering from Gyeongsang National University, Korea. Mr. Kim is currently a Master's Course from Department of Precision and Mechanical Engineering, Gyeongsang National University, Korea.

Youngsu An is an Assistant Professor at the Training Ship Management Center at Gyeongsang National University in Korea. He received his Ph.D. degrees in Fisheries Science from Pukyong National University, Korea, in 2003. Dr. An worked at Gyeongsang National University from 2004 to 2010. Dr. An's research interests include machine diagnosis and prognosis.

ByeongKeun Choi is an Associate Professor at the Department of Energy and Mechanical Engineering at Gyeongsang National University in Korea. He received his Ph.D. degrees in Mechanical Engineering from Pukyong National University, Korea, in 1999. Dr. Choi worked at Arizona State University as an Academic Professional from 1999 to 2002. Dr. Choi's research interests include vibration analysis and optimum design of rotating machinery, machine diagnosis and prognosis and acoustic emission. He is listed in Who's Who in the World, among others.